Energy Reports 7 (2021) 607–619

Contents lists available at ScienceDirect

Energy Reports

journal homepage: www.elsevier.com/locate/egyr

Experimental optimization of engine performance of a dual-fuel compression-ignition engine operating on hydrogen-compressed natural gas and Moringa biodiesel

Babalola Aisosa Oni [a,b], Samuel Eshorame Sanni [a,*], Anayo Jerome Ibegbu [c], Ameloko Anthony Aduojo [d]

[a] Department of Chemical Engineering, Covenant University, P.M.B 1023, Ota, Ogun State, Nigeria
[b] Department of Chemical Engineering, China University of Petroleum, Beijing, China
[c] Department of Mechanical Engineering, Madonna University, Elele, Nigeria
[d] Department of Petroleum Engineering, Covenant University, P.M.B 1023, Ota, Ogun State, Nigeria

ARTICLE INFO

Article history:
Received 17 June 2020
Received in revised form 23 December 2020
Accepted 11 January 2021
Available online 21 January 2021

Keywords:
Moringa biodiesel
Compressed Natural gas
Diesel engine
Compression-ignition engine
Hydrogen
Optimum condition

ABSTRACT

Non admixed Natural gas-fuelled diesel engines are usually associated with harsh engine emissions as well as low performances at moderate to high engine loads. However, the use of Moringa biodiesel as additive in hydrogen-compressed natural gas (HCNG) is a viable novel strategy for reducing toxic emissions such as hydrocarbons and nitrogen oxides in CI engines. In this study, five hybrid HCNG–Moringa biodiesel (MB) oil samples labelled A–E were analysed for their abilities to improve the overall performance of a CI engine (Petter PH1W diesel engine). The fuels had a fixed volume by volume hydrogen : carbon ratio of 87:13% respectively, and the HCNG–MB hybrid samples consisted of 0, 5, 7, 10 and 13 %v/v MB for samples A, B, C, D and E, respectively. At higher engine loads (i.e. 58%–100%), the engine performance improved thus giving higher BTEs in the range of 19–33.9% for all the fuel blends relative to the BTE (15.1%–19%) of the unblended HCNG fuel; this confirms the suitability of MB as an additive for improving the brake thermal efficiency of CI engines; there were also reductions in HC, O_2, CO_2, CO and NOx emissions for all the MB–HCNG fuels relative to the case of the unblended HCNG fuel. At optimum condition, the fuel that gave the best results in terms of the aforementioned engine characteristics is the MB–HCNG fuel blend having 10% MB.

1. Introduction

In the past few decades, fossil fuels have remained the most predominantly available energy-fuels (Adt and Swain, 1974). The combustion of these fuels in CI engines release substances such as CO, CO_2, NOx, hydrocarbons, soot, particulate matter, dust and other gases which have severe consequences on the environment (Arat et al., 2013; Jian et al., 2010; Aklouche et al., 2018). Also, due to environmental concerns and energy shortages arising from fossil consumption, efforts are in place towards exploiting alternative fuels for use in CI engines (Aklouche et al., 2018); this is aimed at reducing exhaust emissions with the desire to improve engine efficiencies (Mehra et al., 2017; Alrazen and Ahmad, 2018). According to Malogorzata (2014), Das (1996), the use of CNG in CI engines considerably reduces environmental pollution, engine vibration and noise, with a significant improvement in the engine brake-thermal efficiency (Shrestha and Karim, 1999).

CI engines are known to be compatible with some gaseous fuels and their blends owing to their improved combustion properties when compared to diesel fuels. According to literature, some biofuels mixed with natural gas, release low amounts of NOx, soot, CO_2 and hydrocarbons as products of combustion, whereas, diesel fuelled CI-engines give higher emissions (Sirens and Rosseel, 2000; Luo et al., 2019). CNG is clean compared to diesel fuels. Natural gas is an alternative source of fuel with high octane number. It mixes homogeneously with air, which promotes excellent combustion and high thermal efficiencies when compared to diesel fuels at high engine loads.

Natural gas comprises of methane, ethane propane and other trace gases (Mehra et al., 2017; Alrazen and Ahmad, 2018; Shrestha and Karim, 1999). Due to the chemical structure of natural gas, it has low combustion properties compared to the conventional diesel fuel. The octane rating of natural gas lies between 121 and 129, which is the reason a CNG-fuelled engine

* Corresponding author.
E-mail addresses: babalola.oni@covenantuniversity.edu.ng (B.A. Oni), samuel.sanni@covenantuniversity.edu.ng (S.E. Sanni), ibegbuanayo@madonnauniversity.edu.ng (A.J. Ibegbu), anthony.ameloko@covenantuniversity.edu.ng (A.A. Aduojo).

https://doi.org/10.1016/j.egyr.2021.01.019

gives high compression ratios as imposed by its high anti-knock properties (Adt and Swain, 1974; Sirens and Rosseel, 2000; Orhan et al., 2004). Natural gas mixes and burns in air. It can be injected directly into the cylinder of a CI engine prior to the end of its compression stroke (Malogorzata, 2014; Das, 1996), thus providing efficient combustion, good fuel economy (Luo et al., 2019; Orhan et al., 2004) as well as power output and thermal efficiency sustenance for an equal amount of diesel fuel (Sierens and Verhelst, 2001). Conversely, injection of CNG directly into a CI engine requires the use of some sophisticated high-pressure injectors. Most of today's applications, require that natural gas or its blends are injected in the intake manifold of an engine in order to uniformly mix it with air, after which it is immediately introduced in the cylinder in order to abate engine-suction loses (Francfort and Karner, 2006; Renny and Janardan, 2008). Natural gas fuelled internal combustion engines usually encounter difficulties such as lean burn-rates, low flame speed and low methane ignitability. These shortcomings may also result in longer combustion durations, lower power outputs and high combustion-cycle variations (Kahraman et al., 2009; Zhang et al., 2016; Park et al., 2012).

Research has shown that hydrogen can either be used as a substitute fuel source (Anon, 2014) or in compressed form with natural gas. The recent use of hydrogen compressed natural gas, rather than natural gas, as fuel source in CI engines, is borne out of the fact that hydrogen (H_2) gas gives better combustible properties such as low ignition energy, wide flammability limits, high flame speed, and less emissions. Also, awful experiences and difficulties, such as, cold wall quenching, vapour lock, poor vaporization and mixing, are usually associated with liquid fuels, whereas, this is not the case with H_2 because, it burns as a clean fuel (Renny and Janardan, 2008; Park et al., 2012; Montoya et al., 2016). When H_2 is burnt, it does not produce noxious products or HC, CO, CO_2 and organic acids; rather, it produces water as its main product. Due to its positive effect on global warming and the advocacy towards sustainable global health, the use of hydrogen as fuel has spurred research interests because of its zero CO_2–emission tendencies (Alrazen and Ahmad, 2018; Francfort and Karner, 2006).

Adt and Swain (1974) determined the emission and performance characteristics of a multi-cylinder engine operating at 50% load with methanol and hydrogen as fuel. The results revealed that the engine BTE fuelled by H_2 was higher compared to the methanol-fuelled engine; the NOx emissions of the hydrogen-fuelled engine were also lower than that of the methanol-fuelled engine. One way of modifying/improving the properties of natural gas is by blending it with H_2 in different proportions (on energy or volume basis) (Renny and Janardan, 2008; Orhan et al., 2004; Boretti, 2020; NGV Global, 2019). The resulting mixture is termed hydrogen-compressed natural gas (HCNG) (Jian et al., 2010; Malogorzata, 2014; Das, 1996; Montoya et al., 2016). Hydrogen as an additive in natural gas helps to improve the overall flame intensity which in turn gives improved combustion and lower emissions. 30% Hydrogen–CNG mixture, improves the combustion properties of NG as well as other performance benefits including high power-output, BTE, low amounts of HC, CO_2, CO, as well as high NO emissions (Shrestha and Karim, 1999; Renny and Janardan, 2008; Boretti, 2020). For increased volume of hydrogen, the lean operating limit extends and the mean brake torque drops. The performance properties of the engine such as spark timing, engine power, thermal efficiency and engine torque depend on the quantity of H_2 blended with natural gas and lambda, which is a measure of the amount of oxygen emission and the compression-ratio of the engine (NGV Global, 2019; Swain et al., 1993). HCNG increases the effectiveness of an engine as well as its combustion potential. HCNG enhances the benefits of compressed natural gas due to the presence of hydrogen (Sierens and Verhelst, 2001; Carlucci et al., 2008). Combustible hydrogen gives varying high flame speed and ignition ranges which has opened-up opportunities for mixing H_2 with CNG even in inadmissible quantities (i.e. 5%–30% H_2) by volume for application in diesel engines (NGV Global, 2019; Yousefi et al., 2019).

The practical limits of CNG- H_2 blends, reported by several researchers, indicate that higher percentages i.e. $\geq$ 19% hydrogen are not recommended for CNG because, it may result in CH_4-loses as high as 86.3% owing to the low Reid vapour pressure imposed by H_2 on the fuel, which may subsequently result in engine power losses; moderate CH_4 loses have also been recorded for 11% H_2 in CNG (Sierens and Verhelst, 2001; Kahraman et al., 2009). In addition, 30% hydrogen to CNG blends can lead to engine-knock (Zhang et al., 2016; Swain et al., 1993; Carlucci et al., 2008).

Sierens and Verhelst (2001), made separate mixtures of 10 and 20% v/v H_2 and compressed natural gas. They recorded higher performance and enhancement for the compressed fuels in terms of thermal efficiency and power, however, the NOx emissions were also high due to the availability of oxygen in the hydrogen-lean mixtures. Renny and Janardan (2008) studied a 3-wheeler engine fuelled with HCNG blends. The engine showed a consistent and safe operation for the blends. Their report demonstrated that H_2 in 21–29 vol/vol CNG gave the best engine efficiency/performance with permissible levels of emissions. In addition, they concluded that the fuel conversion efficiencies improved by 21%–26% for the 14% H_2 + CNG mixture compared to that fuelled by CNG only. Based on the investigation carried out by Jian et al. (2010), the replacement of natural gas (NG) with HCNG gave an appreciable effect on engine efficiency. The experimental results showed that the maximum heat release rate (HRR) and maximum cylinder gas pressure, increased with an increase in the percent hydrogen used. Several researchers have reported low amount of CO_2, HC and CO emissions from HCNG fuelled engines. However, they recorded increased NOx emissions. Swain et al. (1993) demonstrated the performance of a 6-cylinder engine, with 18% H_2 in the HCNG blend. The report showed a decrease in CO by 38%, 25% for HC and 25% for CH_4emissions. However, there was about 32% increase in NOx emissions when compared with those obtained for the CNG fuel. In lieu of this, a high percentage of H_2 (i.e. up to about 30%) in CNG, may cause engine knock (Jian et al., 2010; Renny and Janardan, 2008). Montoya et al. (2016) recorded a decrease in hydrocarbon and CO whereas, the NOx emissions were high at the modest substitution of compressed natural gas with hydrogen. Orhan et al. (2004), adopted a full-load, one-cylinder low-compression HCNG fuelled engine. The recorded thermal efficiency increased with an increase in $\%H_2$ in the fuel blends, but decreased when the $\%H_2$ in the fuel-blend was > 21 percent v/v of CNG. This was due to the high in-cylinder temperature, which caused higher heat losses as well as limited knock spark-timing. At full load, the power output of the engine increased when the %hydrogen in the fuel blend was below 20%. Sirens and Rosseel (2000), pointed out HCNG fuel blend with 30% volume H_2 as being responsible for optimal engine performance; hydrocarbon and carbon monoxide reductions were complemented by a substantial reduction of more than 10% carbon dioxide. According to Luo et al. (2019), the mixing of hydrogen and natural gas increases the burning velocity of the mixture and fuel-combustion, thus reducing the engine's break-specific thermal efficiency (BSFC). At high excess air ratio and spark timing, the BTE increases. The result showed high NOx emission, due to the presence of hydrogen that increased the combustion temperature.

Addition of H_2 to CNG may result in extended flammability, shorter burning time and leaner limits of the mixture. Challenges associated with HCNG as fuel in CI engines are imposed by high

Table 1
Composition of the natural gas.

Composition	v/v (%)
(CH_4)	98.0
(C_2H_6)	0.59
(C_3H_8)	0.21
(C_4H_{10})	0.20
(C_5H_{12})	0.1
(CO_2)	0.1
(N_2)	0.8

Net heating value = 48.6 MJ/kg.

H_2/CNG ratio. Owing to the slight decrease in the brake specific fuel consumption and power output of the engine at full load, it becomes necessary to apply caution in designing HCNG storage and supply infrastructures (Swain et al., 1993; Yousefi et al., 2019; Papagiannakis et al., 2010; Srinivasan et al., 2007). To overcome these drawbacks, Moringa biodiesel was introduced into HCNG for use in a CI engine. Several blends of HCNG and MB were tested in order to ascertain the best blend for optimum engine performance, good combustion and reduced emissions, especially with respect to NOx gases. Moringa biodiesel is nonexplosive, it is renewable, biodegradable, nontoxic, has high flash point, excellent lubricity and is environmentally friendly. This oil possesses significant resistance to oxidative degradation (Orhan et al., 2004; Anon, 2014; Boretti, 2020; Zheng et al., 2019). The seed contains 38%–40% oil. About 39%–43% oil yield can be obtained via hexane-extraction. Its protein, fibre and ash contents are in the range of 28.5–31, 5.9–9.19 and 5.7–8.5%, respectively (Wang et al., 2018; Niju et al., 2018; Ali et al., 2018; Boretti, 2018). Carlucci et al. (2008), reported that oil extracted from Moringa seeds amounts to 36 percent w/w of crude Moringa oil.

To date, there is no existing literature that bothers on the use of Moringa biodiesel and hydrogen compressed natural gas as fuel blends for CI engines; this then gave the motivation for this study. In addition, the experimental optimization of the blended Moringa fuel and hydrogen compressed natural gas was carried out in order to ascertain the best fuel combination for optimum engine performance, which in turn helps to conserve useful resources as well as provide sustainable energy; this also has not been considered by previous publications on the subject. Also, due to the fact that no literature has reported the consideration of Moringa seed oil as a blend for hydrogen compressed natural gas for use in CI engines, several blends of the oil were mixed with different proportions of HCNG in a bid to find out the blend that will give high CI engine performance, good combustion properties and, minimal emissions.

2. Materials and method

The natural gas used in this study was supplied from Nigerian gas company (NGC), limited, Warri, Nigeria, with composition as stated in Table 1.

H_2 gas from a high-pressure vessel was supplied to an electromagnetically actuated gas injector (supplied by BOC gas company limited, Oshodi, Lagos, Nigeria), and a mass flow controller was used to measure the hydrogen flow-rate. H_2 was stored at 200 bar in a high-pressure storage tank, and regulated by a stainless-steel double stage pressure regulator. The hydrogen passing through the regulator was passed through a shutoff valve. Pressure relief-valves were used to prevent overpressure; furthermore, pressure gauges were connected to display the line pressure. A thermal mass-flow meter calibrated to meter H_2 flow in methane, was used for the flow measurement. The H_2 flow fluctuations were controlled with a buffer tank. Table 2 shows the composition of H_2 and CNG adopted for this study.

Table 2
CNG and H_2 Composition.

Chemical structure[a]	Natural gas	Hydrogen
Hydrogen to carbon ratio	4:1	0
Energy density(MJ/kg)	48–50	120
Auto ignition temperature (K)	813	858
Minimum ignition energy (ml)	0.29	0.02
Octane rating	120+	130+
Flammability limits (%)	5.3%–14%	4%–70%
Stoichiometric Air–fuel ratio	9.48	29.53
Wobbe index, MJ/Nm^3	47.91–53.28	40.65–48.23
Flame velocity in air at NTP, cm/s	37–45	265–325
Flame temperature (K)	2148	2318
Density (g/L)	0.7	0.07
Emissions	HC, CO, CO_2,NO_2, CH_4	H_2O, NOx
Energy Density MJ/Lts	25.3	2.9 at 350 bar

[a]NTP = normal temperature and pressure.

Chemical or solvent based method of extraction was used to extract oil from Moringa seeds because, the screw press method adds to the overhead cost of the extracted oil. Moringa oleifera oil seeds contain 32%–40% w/w oil yield. Several factors such as solvent type, extraction time, and solid to solvent ratio determine the efficiency of the extraction process. The Soxhlet extractor was used to extract oil from 500 g of crushed Moringa seeds; 1 litre of hexane was used as solvent and the extraction process lasted 5 h. At 45 °C, the solvent was evaporated from the rotary evaporator under vacuum conditions giving 36% w/w yield of oil. 150 g (Moringa Oleifera oil) was trans-esterified with 1 weight percent $NaOCH_3$ catalyst and 5:1 methanol to oil molar ratio for 1 h at 60 °C. Impurities such as glycerol, unreacted catalyst and excess methanol settled at the base of the separating funnel, while the methyl esters were collected at the top of the funnel. The properties of the characterized Moringa biodiesel are as illustrated in Table 3, and Table 4 shows the Moringa oil fatty acids

2.1. Blending of HCNG with Moringa biodiesel

The blending of the fuels (HCNG and MB) was initiated by first injecting the fuels in the homogenizer/agitator via two feed pots i.e. the homogenizer has two feed pots for fuel intake; one nozzle for the HCNG (lighter fluid) which is located at the bottom, and another for the biodiesel (denser fluid) which is located at the top of the homogenizer. This is to enable proper mixing before intake/injection and compression and not at the compression stage. The HCNG and Moringa biodiesel were agitated for 20 min at 2500 rpm. The HCNG injector used is the BRC Italy of supply voltage 8–16 V, peak current 4 A, holding current 1 A, flow capacity 0.8 g/s at 4 bar, working pressure 103–552 kPa and maximum rail pressure of 4 bar.

Note: hydrogen is lighter and tends to rise to the top of the homogenizer while the denser MB will tend to displace hydrogen from the bottom section of the homogenizer; hence, with the help of the agitator, the fluids interact and mix which ensures more mixing than separation.

Five fuel samples consisting of a fixed hydrogen to methane ratio (87:13) were selected for experimentation with a Petter PH1 W diesel engine after several trials. The mixtures: 100% HCNG or 87:13 H_2:CNG containing 0, 5, 7, 10 and 13% v/v of Moringa biodiesel were labelled A, B, C, D and E, respectively. The proportion of hydrogen, CNG and MB in the different fuel blends were calculated and the data is contained in section A.1 of the Supplementary file.

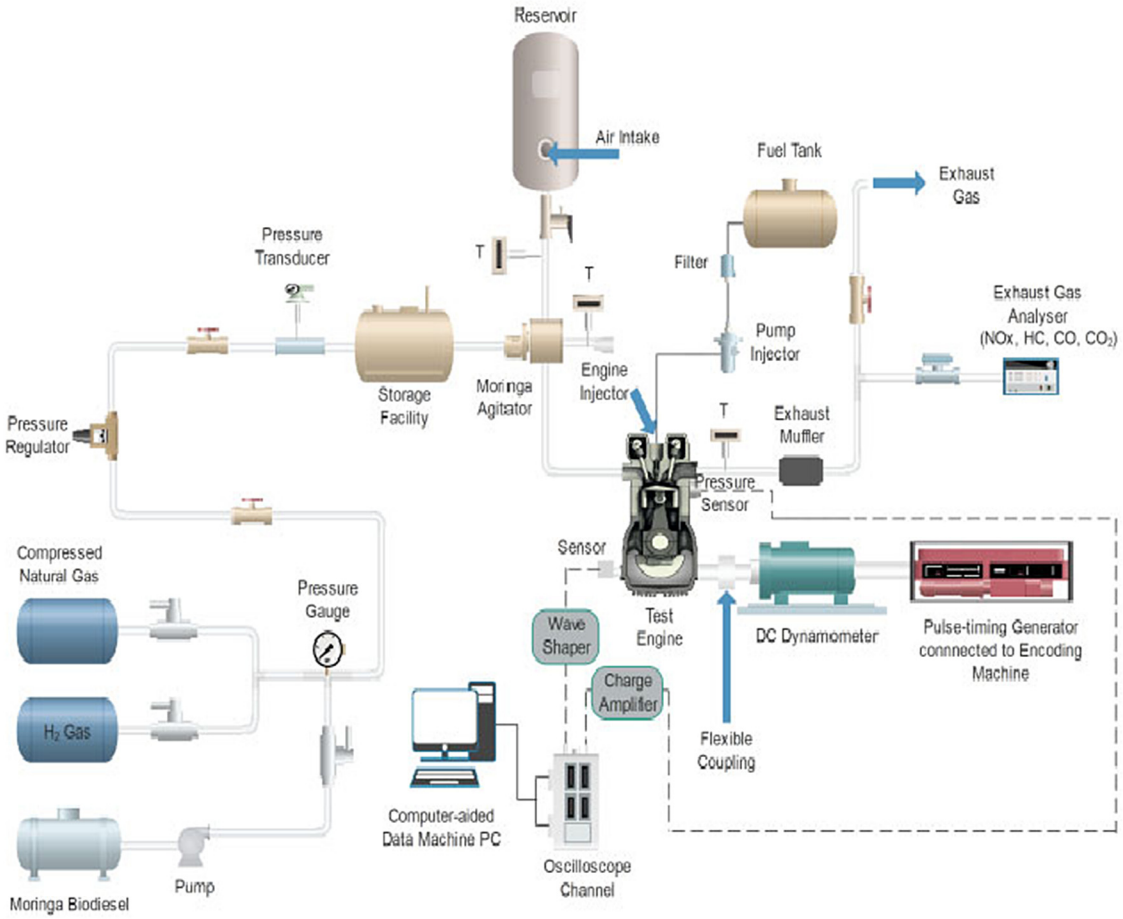

Fig. 1. Schematic of test engine.

Table 3
Characteristics of the Moringa biodiesel.

Parameter	Units	Moringa biodiesel
Density	kg/m^3 or g/L	882
Flash point	°C	168
Kinematic viscosity	mm^2/s	4.34
Pour point	°C	17
Cloud point	°C	8
Cetane number		67.04
Cold filter plugging point	°C	18
Higher heating value	MJ/kg	39.05
Oxidative stability	H	3.71
Lubricity	HFRR; μm	139
Dynamic viscosityAuto ignition temperature	mPa.s°C	4.78525 (798 K)

The cetane number of the biodiesel was determined using ASTM D613 procedure.

Table 4
Moringa oil fatty acids.

Fatty acid	Chemical name	Structure	Moringa oil
Palmitic	Hexadecanoic	16:0	6.5
Palmitoleic	9-hexadecanoic	16:1	2.0
Stearic	Octadecanoic	18:0	6.0
Oleic	Cis-9-Octadecanoic	18:1	72.2
Linoleic	Cis-9, cis-12-Octadecanoic	18:2	1.0
Arachidic	Eicosanoic	20:0	4.0
Gadoleic	11-eicosanoic	20:1	2.0

2.2. Engine test

In Fig. 1, 87% of 109 L (H_2) and 13% of 109 L (HCNG) were transported separately from the hydrogen and CNG banks via a flow line. Flow rates of the gases were measured using flow meters. After transporting the gases to the homogenizer, the gases were then mixed in the homogenizer at 2500 rpm. Thereafter, using the HCNG injector, the 100% HCNG was then injected using the BRC Italy HCNG injector to inject the fuel into the engine. The engine was then run on HCNG only. Afterwards, 87% H_2 and 13% CNG were again transported to the homogenizer from the hydrogen and CNG storage tanks. For this second operation 5% v/v MB was pumped to the homogenizer where the entire mixture was homogenized/mixed properly. Thereafter, the HDP6 Bosch Mobility Solutions high pressure injector with operating pressure limit of 350 bar, delivery capacity of 0.9 cm^3/rev (146 L/h), piston diameter of 8 mm and single cylinder pump was used to transfer the hybrid fuel into the engine cylinder whose air to fuel ratio = 17.2:1. Subsequently, the last step was repeated

Table 5
Specifications of the engine.

Brand	Petter PH1W diesel engine	
Engine specification	4-stroke, constant speed, Single cylinder, compression ignition, water-cooled, inter cooler, naturally aspirated, vertical.	
Compression ratio	17.5:1	
Clearance volume	39.9 cm^3	
Bore	87.3 mm	
Rated power and Speed	8.2 bhp @ 2500rpm	
Stroke	110 mm	
Injection pressure	200 bar	
Fuel injection System	Direct injection (DI)	
Swept volume	659 cm^3	
Nozzle hole diameter	0.3 mm	
Valve timing:	when opening	when closing
Intake	4.5° BTDC	36.5° ABDC
Exhaust	5.5° BBDC	4.5° ATDC
Spray angle	120°	
Number of nozzle holes	3	

for the 7, 10 and 13% MB and the engine characteristics were determined; the volume of Moringa biodiesel used correspond to 0% (0 L), 5% (4.58 L), 7% (6.4 L), 10% (9.17 L) and 13% (11.9 L). The engine considered for this research is the Petter PH1 W diesel engine (Fig. 1) with its specifications given in Table 5. In order to visualize the effects of Moringa biodiesel addition to the HCNG in the engine, the experiments were conducted at full load (100%) condition and the engine's emission, performance, and combustion characteristics were determined. Also, the engine load was later varied for the different fuel blends at different operating loads in order to ascertain the effect of load variation on the engine characteristics, the results are presented in a later section. A piezoelectric transducer (Kistller 60052A) was used to observe the in-cylinder pressures. Since the ignition delay is paramount to combustion and engine performance, the ignition delay of the engine was measured at the initiation step/startup of the combustion process. The measured in-cylinder pressures were used to compute the HRR based on the first law of thermodynamics (see Eq. (1)), temperature dependency of the specific heat of the mixtures and the heat loss to the combustion chamber wall. A pressure higher than 7 MPa in the cylinder may affect the gas injector, when the injection pressure is set at 8 MPa. The devices/instruments used in taking measurements, their absolute errors and uncertainties are as given in Table 6. Although the experimental test engine was operated at constant load condition while testing the effect of other parameters, however, the authors were curious in determining the effect of varying engine load on the performance (BTE) of the engine for the blended fuels, hence, in order to satisfy that quest, the engine was run at different loads by adjusting the engine load-control knob between 20 and 100%; the results are discussed in a later section.

$$\frac{dQ}{dt} = \frac{\gamma}{\gamma - 1} P \frac{dV}{d\theta} + \frac{1}{\gamma - 1} V \frac{dP}{d\theta} \tag{1}$$

$\frac{dQ}{dt}$ = change in heat release rate with time; γ = Cp/Cv (ratio of specific heat capacity at constant pressure to the specific heat capacity at constant volume, approximately = 1.4), in-cylinder pressure = P, V = volume of fuel.

According to Ağbulut et al. (2019), Eqs. (2)–(5) can be used in estimating the emission concentrations for CO, O_2, HC and NOx in g/kWh. Eqs. (2)–(5) were used to determine the emissions in terms of mass of emitted component per energy of fuel consumed and the results can be seen in Tables A.1–A.4 in section A.2 of the Appendix of the supplementary file.

$$\mathrm{CO}\left(\frac{g}{kWh}\right) = 3.591 \times 10^{-3} \times CO(ppm) \tag{2}$$

$$\mathrm{HC}\left(\frac{g}{kWh}\right) = 2.002 \times 10^{-3} \times HC(ppm) \tag{3}$$

$$\mathrm{NOx}\left(\frac{g}{kWh}\right) = 6.636 \times 10^{-3} \times NOx(ppm) \tag{4}$$

$$\mathrm{O_2}\left(\frac{g}{kWh}\right) = 41.024 \times O_2(Vol.\%) \tag{5}$$

2.3. Instrumentation and uncertainty measurements

Prior the experiments, all instruments/equipment were calibrated according to the manufacturers' instructions. However, the experiments were done in triplicates within the standards presented, and the average values were taken within the specified absolute errors, accuracies and uncertainties as presented in Table 6. Also, in order to ensure that the accuracies of the measured values are high, the gas analysers were calibrated before each measurement using reference gases. The smoke meter was also allowed to adjust to its zero point before taking each measurement. Considering the results obtained, it is quite evident that the measurements are repeatable/reproducible for all measurements.

The instruments used were calibrated, and tested for accurate measurements under the same operating conditions prior to the experiments. The gas analysers used were purged after each measurement; calibrations of the gas analysers were done before taking measurements with the equipment. Furthermore, the experiments were conducted three times to ascertain the repeatability of the measured values for each parameter. Comprehensive uncertainty analyses were carried out on the basis of the instruments' accuracies and the measured values. Table 6 shows the measurement devices, absolute errors and their uncertainties.

3. Results and discussion

3.1. Combustion properties

The profile of combustion pressure and crank angle relationship is as given in Fig. 2.

Progressive combustion in the engine is one major factor that influences the change in cylinder pressure (Rashed et al., 2016a; Banapurmath and Tewari, 2009; Ghazal, 2013; Lather and Das, 2019) and the crank angle. All the fuel blends show peak cylinder pressures at an approximate angle of 360° with fuel blend D giving the highest (optimum %MB in HCNG) cylinder peak pressure of 79 bar. This is because, the cylinder pressures of all the fuel blends increased in the order of A< B < C < E < D, which implies that beyond 10%MB in HCNG, the cylinder pressure began to drop as observed; this corroborates the findings of other

Table 6
Measurement devices, their absolute errors and uncertainties.

Parameter measured	Measurement Device	Absolute error	Accuracy	Uncertainty
NO	AVL DiCom 4000	1 ppm	1 ppm	±0.2
CO	AVL DiCom 4000	0.002%	0.01% vol	±0.3
HC	AVL DiCom 4000	2 ppm	1 ppm	±0.2
CO_2	AVL DiCom 4000	0.1%	0.1% vol	±0.2
O_2	AS8800L	1 ppm	1 ppm	±0.1
Engine speed	Incremental encoder	0.20 rev/s	1.0	
Engine torque	Load cell	0.6 Nm	2.0	
Inlet air flow rate		0.300 m^3/h		±2
Natural gas flow rate		1.184 E^{-2} m^3/h		±2
Hydrogen flow rate		1.02 E^{-2} m^3/h		±0.2
Diesel fuel flow rate		8.3 E^{-3} kg/h		2.5

AVL (Company trade name), ppm = (parts per million).

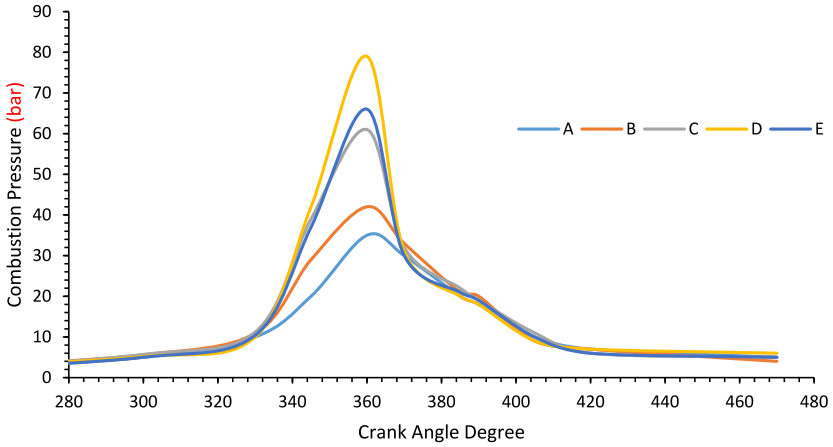

Fig. 2. Variation of combustion pressure (bar) with crank angle.

authors (Sierens and Verhelst, 2001; Carlucci et al., 2008). Beyond a crank angle of 380°, all fuel blends seem to possess near similar cylinder pressures. Also, between 0 and 330°, all fuels had a slow rise in crank case angle and very close cylinder pressure values (Fig. 2). Due to the observed characteristic peak pressures, it can be deduced that the difference in auto ignition temperatures of the hydrogen (858 K with a density of 0.07 g/L), CNG (with an autoignition temperature of 813 K and a density 0.7 of g/L) and moringa biodiesel with an auto ignition temperature of 798 K and average density of 0.882 g/L, would lead to a corresponding rise in the crank angle and pressure with high laminar flame which peaks at the point of instantaneous combustion phasing of hydrogen where the flash point of the biodiesel would have been lowered thus causing the fuel to quickly go into vapour phase.

Also, considering Fig. 3, the HRR (Heat release rate) peaks are in the order described for the profile illustrated in Fig. 2, i.e. A<B<C<E<D with the fuel blend comprising of the 10% MB + HCNG giving the highest HHR of 377 J/°CA. When the Moringa biodiesel–hydrogen fuel blend is below a definite volumetric fraction, the maximum: HRR, mean gas temperature, cylinder gas pressure, and rate of pressure rise decrease, but increase with an increase in the oil fractions (Moringa biodiesel oil) mixed with HCNG. The crank angle of the centre of the HRR curve deviates from the top-dead-centre with an increase in Moringa biodiesel mixed with HCNG when the oil-fraction is less than the optimum volumetric fraction; the CA later moves close to the top-dead-centre when the peak value is attained. The peak cylinder pressure for the Moringa biodiesel and HCNG blends (i.e. samples A, B, C, D and E) are 35, 42, 61, 79 and 66 bar, respectively.

The Combustion intensity and duration are assessed from an engine's HRR, which is very important for understanding the combustion mechanism in CI engines (Nwafor, 2003; Boretti, 2019). The HRR curve reveals the early combustion stage where NOx gases are formed (Shrestha and Karim, 1999). The net HRR is obtained by applying the principles of the first law of thermodynamics. The start of combustion of the blended fuel occurs early as revealed by the rise in the HRR (i.e. early but slow rise in HRR). This may be due to the shorter ignition delay exhibited by the fuel blends. The heat release rate curve is characterized by the occurrence of two peaks; one is for the pre-mixed speedy combustion phase while the other depicts the mixture-controlled/homogeneous mix combustion phase as obtained in Boretti (2020). When the load is at 50%, a minute quantity of natural gas is used up. Based on the results (Fig. 3), the 100% HCNG fuel gave the lowest HRR thus confirming the positive influence of H_2 in the HCNG–biofuel blends. This is due to the lean mixture of gas to fuel and air ratio for small loads and poor fuel consumption efficiency, which makes a large portion of natural gas escape combustion in the combustion chamber; this is also justified by the low heat release rates in Fig. 3. As previously observed, the burning rate of the natural gas was slow. The peak heat release rate for fuel-blends A, B, C, D and E are 71, 76, 78, 79 and 73 J/°CA respectively, thus defining an optimum heat release rate for the 10% MB–HCNG fuel blend. The addition of Moringa biodiesel in the HCNG accelerates the initiation of premix-combustion. When the Moringa biodiesel in the HCNG increases, it enhances the HRR; this is in line with the findings of some authors (Montoya et al., 2016; Carlucci et al., 2008; Zheng et al., 2019).

The interval between the start of combustion and injection initiation is known as the ignition delay of the diesel engine (Orhan et al., 2004). It is also an interval when the first portion of fuel goes into the chamber to the point where the initial flame is detected in the spray. The ignition delay period can be physically or chemically influenced; the former involves vapour mixing of air and fuel after atomization while the latter is ascribed to

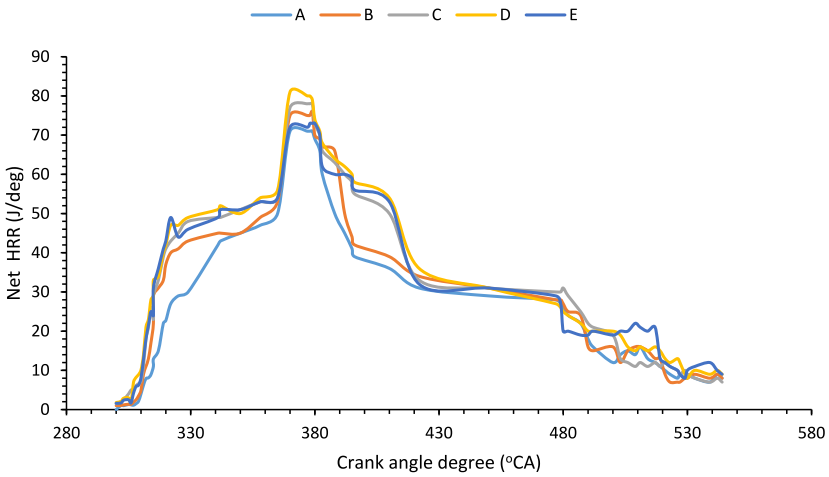

Fig. 3. Variation of Heat release rate (HRR) with the crank angle.

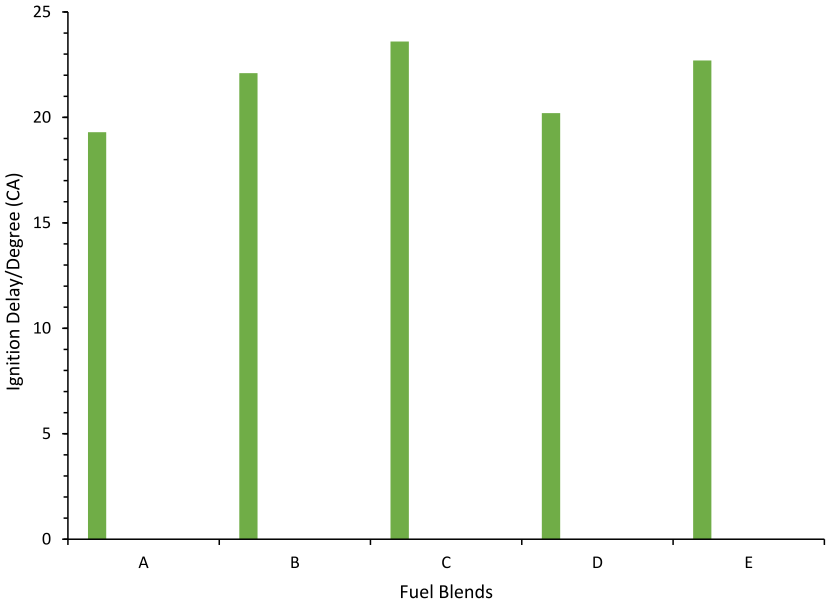

Fig. 4. Ignition delay for the fuel blends.

a pre-combustion condition, however, they both occur concurrently (Malogorzata, 2014; Das, 1996; Zhang et al., 2016; Orhan et al., 2004). For NOx emissions to be reduced, there is need to reduce the ignition delay, especially in modern engines. Ignition delay plays a vital role in combustion processes. This period is usually determined from the change in the slope of the pressure and heat-release plot. The time delay determines the quality of the premixed flame generated (Jian et al., 2010). Factors such as the engine noise, rate of pressure rise, vibrations, mechanical stress, and peak pressure depend on the ignition delay. Generally, factors such as intake air pressure, air–fuel ratio, fuel atomization, fuel type/quality, temperature and engine speed, influence the ignition delay. However, fuel type is the most significant parameter that affects the delay period (Sirens and Rosseel, 2000; Wang et al., 2018). Ignition delay is a function of ambient temperature and pressure. The delay in ignition of a diesel spray is significant from the perspective of formulating the fuel before injecting it into the engine prior to the selection of an optimum injection timing. During the process of ignition delay, the fuel becomes mixed with hot compressed air and vaporizes.

Hence, it is advisable to measure this parameter at the beginning/initiation of the combustion process, hence the ignition delay was measured at the beginning of the combustion process. After ignition delay, spontaneous ignition of the fuel occurs. The addition of Moringa biodiesel to HCNG controls the ignition delay between the start of combustion and the commencement of gas-injection. In spite of the higher cetane number of the blends relative to that of the unblended fuel, when the concentration of the blends increases, ignition delay decreases due to reduced formation of ignition centres inside the combustion chamber. This is attributed to high oxygen content, dense mixture, high viscosity, and heavy molecular structures of the fuel blends, which reduce the rate of mixing and evaporation of the MB + HCNG fuel blends. As observed, Moringa biodiesel reduces the NOx emissions, by reducing the ignition delay period, this agrees with the results of some authors (Yousefi et al., 2019; Srinivasan et al., 2007). Fig. 4 shows the variations of the ignition delays of the fuel blends A, B, C, D and E, whose corresponding values are 19.3, 22.1, 23.6, 20.2 and 22.7 /°CA respectively; again, considering the fuel blends, the optimum ignition delay can be pegged at 20.2 /°CA which still draws one's attention to the fuel blend comprising of 10% MB–HCNG. Also, it is important to note that the properties reported in Figs. 2–4 were for data measured at full load condition, whereas, at varying engine load, the properties

measured include the engine's BTE and exhaust gas emissions as discussed in the following sections.

3.2. Performance property

Fig. 5 shows the BTE at full load for the dual-fuel blends A, B, C, D, and E respectively. BTE shows how effective a fuel is burnt in the combustion chamber for subsequent conversion of heat to work. An increase in BTE of the dual fuel systems resulted in low brake specific fuel consumption (BSFC) and increased BTE up to the optimum point which is characterized by the fuel blend with 10% biodiesel in HCNG; the BTE of sample D is 33.9% as compared to 19% for the unblended HCNG, this gives about 78.4% increase in BTE.

Those of samples E, C and B, are 32, 31 and 29 respectively, which give corresponding BTE increase of 68.4, 63.2 and 52.6% respectively. When the compression ratio is increased, it definitely increases the engine efficiency. The dual fuel engine then takes in less fuel due to the high calorific value of the natural gas which aids the complete combustion of the fuel system. High calorific value, kinematic viscosity, cetane number and low oxygen content, are all inherent properties of the fuel, which also have effects on the BTE. Generally, the lean mixture of the gaseous fuels and the low fuel efficiencies of about 33.9% can be as a result of the imposed low BTE of natural gas. Factors such as high self-ignition temperature and low cetane number of natural gas give rise to sudden decrease in the burning rate of the combustion process thereby increasing the ignition delay period (Orhan et al., 2004; Boretti, 2020). At low to medium engine loads, there is a decrease in the BTE which increases the brake specific fuel consumption with a subsequent rise in the cylinder temperature at high engine loads. Alternatively, an increase in the brake thermal efficiency caused by mixing HCNG and Moringa biodiesel gives rise to a higher cetane number and controlled self-ignition temperature as highlighted in Montoya et al. (2016), Srinivasan et al. (2007) and NGV Global (2019). Therefore, the rate of combustion increased with BTE and the BTE of A at full load was lowest with 19%, while D has the highest BTE of 33.9% at full load.

3.3. Emission properties

The variation of unburned HC is illustrated in Fig. 6 as emission index (EI-HC). The HC released from the blended fuels were lower relative to the HCNG unblended fuel. Again, it is important to note that the fuel with 10% MB gave the least HC emissions. The variation of unburned HC in the exhaust is steady with the quality of combustion in the engine; this is corroborated by the fact that hydrogen and carbon are the main fuel elements in the fuel blends (Carlucci et al., 2008). HC emission occurs due to incomplete combustion of fuel inside the combustion chamber. As the engine load increases, the HC emission decreases. This may be due to an increase in gas temperature that helps to oxidize the unburnt HCs. Also, in the course of the experiment, the addition of Moringa biodiesel in the HCNG was also responsible for the sharp drop in the amount of HC emissions. Thus, the air/fuel admix-temperature at the walls of the combustion chamber is considerably less than the temperature at the centre of the chamber, thus emitting low amounts of HC. Unburnt hydrocarbons may also react in the exhaust chamber at 700 °C in the presence of oxygen. Hence, emissions of hydrocarbon from the tailpipe will be lesser than emissions from the cylinder. Hydrocarbon emissions also occur during the atmospheric venting of vapours from the fuel system throughout the fuel dispensing and distribution stages, as well as in the engine's crankcase. Certain factors, such as, engine design/adjustment and fuel type, affect the hydrocarbon content of the fuel. Injector needle vibration, dynamics in engine speed, untidy injection, and excessive nozzle cavity volumes cause the passage of high amount of unburnt fuel through the exhaust. With the addition of Moringa biodiesel, there is a significant decline in hydrocarbon emissions of the fuels as shown in Fig. 6.

In Fig. 7, at maximum load of 100%, it is clearly evident that the fuel blend comprising of 10% MB gave the lowest NOx gas emissions ranging from 5.01–3.77 g gas/kg diesel. This goes further to say that it is an excellent reducer of NOx emissions (i.e. by about 76.4% as compared to the unblended HCBG fuel). Nitric oxide formations in the combustion chamber occur due to the Fennimore and thermal mechanisms or the Zeldovich mechanism. Thermal mechanism is associated with high-temperature formation of NO during combustion, especially at temperatures above 1400 K. Here, the NO formation rate exponentially increases with an increase in the combustion temperature. Conversely, the mechanism that prompts NO-formation occurs inside the rich-low-temperature regions. In this region, active radicals are available. Fig. 7 defines the (NO) emissions for different engine loads. Formation of nitrogen oxides is favoured by high charge temperature and high concentration of oxygen. The concentration of nitric oxides is affected by the presence of gaseous fuel in the charge mixture. An increase in combustion duration, cylinder temperature and oxygen concentration result in an increase in the NO emissions. Nitric acid concentration under mixed fuel mode is relatively low due to the low rate of pre-mixed controlled combustion of the gaseous fuel which gives rise to a low charge temperature within the combustion chamber. At high engine load, the concentration of nitrogen oxide under mixed fuel operation is low due to the less intensity of pre-mix combustion at low temperature; it may also be as a result of the high amount of gaseous components in the blends. Therefore, an increase in the engine load under dual fuel operation causes a decrease in nitrogen oxide emission which occurs as a result of an increase in the burnt gas temperature that helps to efficiently oxidize the unburnt HCs. In addition, the inclusion of Moringa biodiesel in the HCNG was also responsible for the sharp drop in the NOx emissions; this is in agreement with the findings in Kahraman et al. (2009), Park et al. (2012), Orhan et al. (2004).

The release of CO_2 from combustion engines contributes to the volume of global warming and greenhouse gases in the atmosphere. High CO_2 release corresponds to increased engine load, but for the fuels, lower CO_2 emissions were recorded as compared to those obtained for the unblended HCNG fuel. At full load condition, fuel samples D and E gave close CO_2 emissions i.e. approximately 2020 g CO_2/kg MB–HCNG mix with sample D giving the least CO_2 emission, ranging from 1750 at 20% - 2020 g/kg diesel at 100% engine load; the unblended HCNG fuel gave 2520 g CO_2/MB–HCNG emissions, which gives a difference of 500 g/kg MB–HCNG. High human exposures to CO_2 can lead to severe health consequences including high blood pressure, convulsions, asphyxia etc. An increase in engine load, increases the CO_2 emission from the MB biodiesel–HCNG fuels, as illustrated in Fig. 8. Complete combustion in the combustion chamber increases the CO_2 emissions rapidly. However, this depends on the operating conditions of the engine and the fuel used in running the engine. The additional oxygen present in the blends resulted in the oxidation of carbon monoxide to carbon dioxide (Srinivasan et al., 2007). The CO_2 emission decreased by 11.9% for fuel-sample D, it is 9.5% for sample E and 8.7% for samples C and B when compared with the CO_2 release rate of the unblended HCNG sample (sample A). In lieu of the fact that the Moringa plant would have trapped CO_2 during photosynthesis, it is clear that the resulting fuels were unaffected by the carbon dioxide intake during the growth phase of the plant. Furthermore, the fuel-blends had a lower percentage of unconverted CO, thus resulting

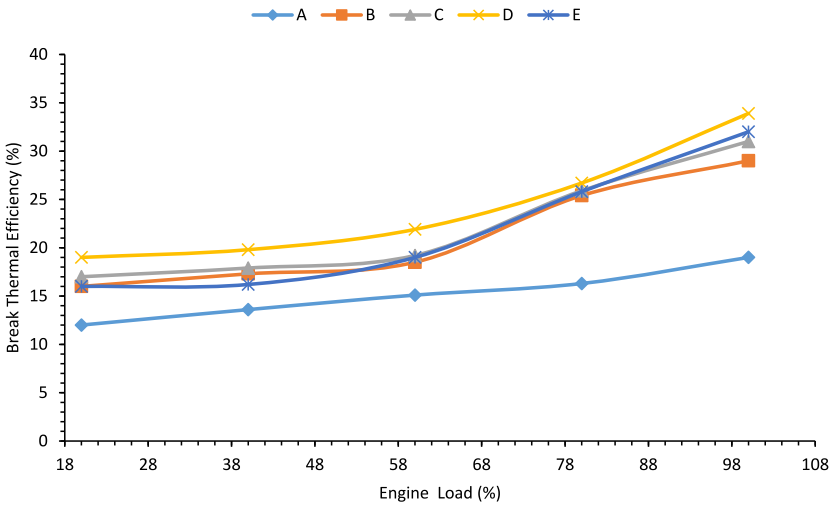

Fig. 5. Brake thermal efficiency versus engine load.

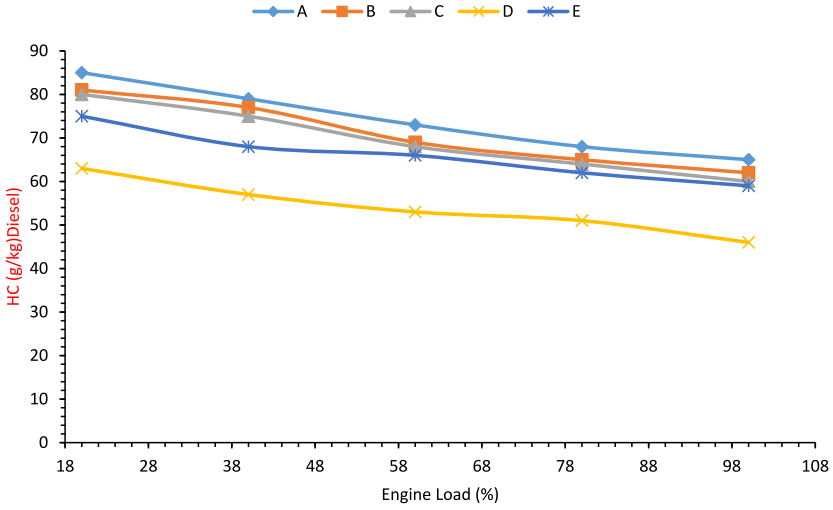

Fig. 6. Unburnt hydrocarbon concentration vs engine load.

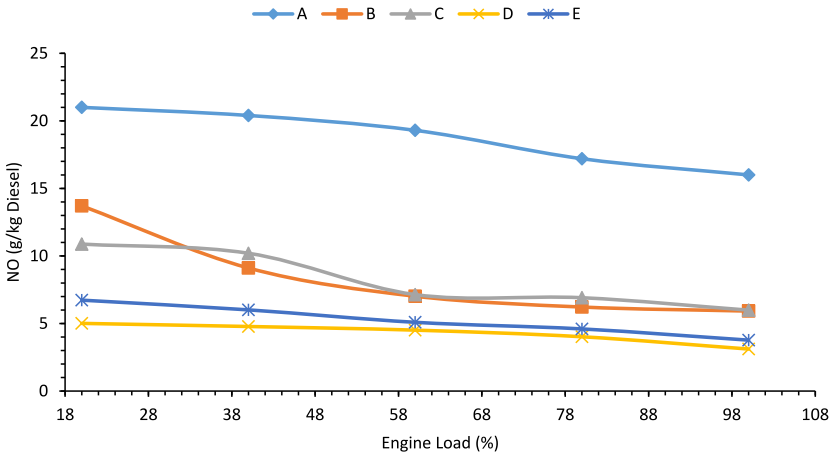

Fig. 7. NOx concentration vs engine load.

in a low amount of carbon dioxide emissions. Also, the lower tendencies for oxygen in the biodiesel molecular structure can be seen to be the possible reason for the lower amount of its carbon dioxide emission compared to HCNG when they were combusted as fuel.

The formation of CO occurs due to incomplete combustion of the gaseous fuel available at the combustion temperature of the mixture. This controls the rate of fuel oxidation and decomposition. The amount of CO under mixed fuel operation decreases with increase in the engine load for samples A–E.

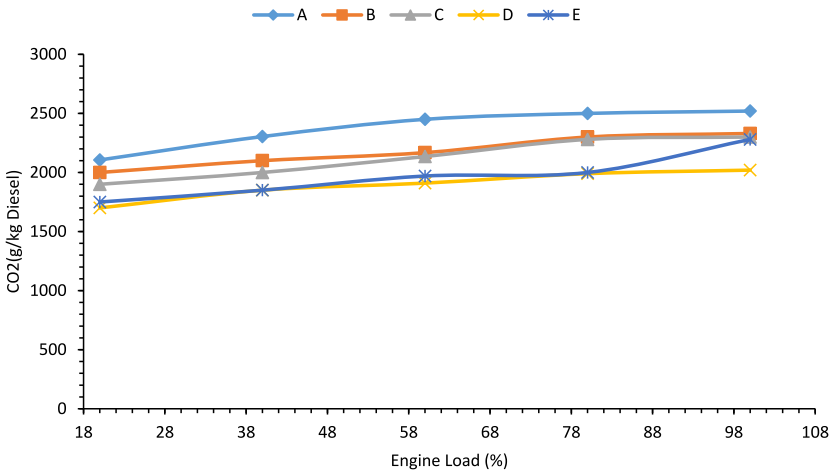

Fig. 8. CO_2 concentration vs engine load.

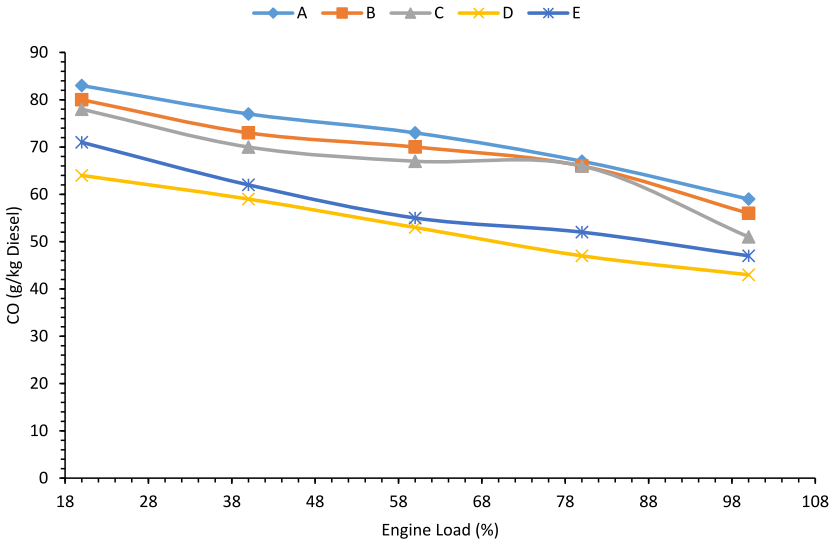

Fig. 9. CO concentration versus engine load.

Again, at maximum load condition, sample D gave the least CO emissions compared to other samples; the 10% MB–HCMG sample/sample D reduced the CO emission by 27% when compared to the CO emission of the sample without MB (Fig. 9). This occurs due to the enhancement of gaseous fuel utilization, specifically during the combustion process. When the engine load is relatively high, the rise in engine load may not affect CO concentration, due to shorter combustion time. The carbon monoxide reduction in the exhaust gas indicates that complete combustion can be achieved (NGV Global, 2019). When the CO concentration in the exhaust gas is low, better combustion is achieved. During the burning of hydrocarbons, CO is formed in the process. Most of the CO is subsequently oxidized to CO_2 during the power and exhaust strokes. When oxygen is sufficiently available at high exhaust temperatures, CO immediately becomes converted to CO_2 leaving behind small concentrations of CO in the exhaust. The occurrence of CO depends on the nature of the post oxidation reactions. In diesel engines, the carbon oxidation reaction is partially complete due to the occurrence of excess air. CO is not formed until the smoke limit is attained. Higher emissions of CO from the mixed fuels, reduce the mean effective pressure and adiabatic flame temperature, which justifies the findings of some authors (Shrestha and Karim, 1999; Park et al., 2012; NGV Global, 2019; Niju et al., 2018; Boretti, 2018).

When an excess quantity of air is used to burn some amount of fuel in a CI engine, some of the oxygen present in air oxidizes the fuel, while a large quantity of the oxygen diffuses through the exhaust pipe. Also, some air farther away from the combustion region, may not be combusted and thus escape as unburnt air through the exhaust. Fig. 10 shows the concentration of oxygen in the exhaust tailpipe for the mixed fuels. The results show that the decline in the amount of oxygen for all the fuels, is in the order of D< E<C<B for the MB–HCNG fuel blends with sample A giving the highest amount of oxygen release at all engine load conditions. At 31% engine load, sample D gave 45% reduction in oxygen emission as compared to the HCNG unblended fuel. The oxygen concentration at the exhaust reduced for all the blended fuels due to a large amount of fuel utilization in the cylinder. The concentration of oxygen in the exhaust gas is a measure of the cylinder charge-voidage. Thus, the oxygen content of the charge reduces the oxygen concentration in the exhaust gas. The quantity of gaseous fuel that interacts with the oxygen is very small when compared with the quantity available in the cylinder section.

In Fig. 10, the engine variation for oxygen emission was maximum at 31% not 33%. However, it was noticed that at higher engine loads than 31%, the exhaust was no longer delivering significant or measurable amount of oxygen, hence no readings

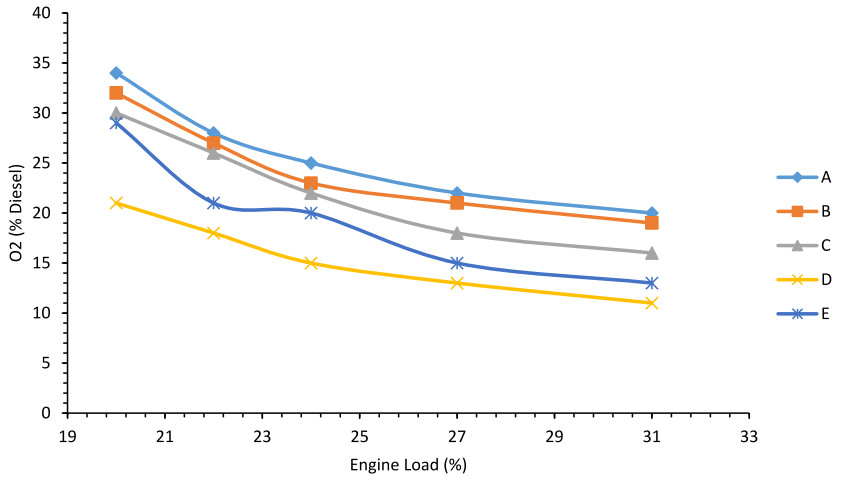

Fig. 10. Oxygen concentration vs engine load.

Table 7
Properties of the HCNG-10%MB fuel with other fuels.

Fuel	Cetane number	Ref.
Conventional diesel	48, 46	Anon (2020), Atabani et al. (2013)
Moringa oil	67, 67.04	Atabani et al. (2013), This work
Beauty Leaf Oil (BLT)Palm oil	57.352	Atabani et al. (2013)
HCNG+10%MB	50	This work

were recorded by the oxygen analyser (AS8800L) and since, the amount of oxygen delivered at the exhaust of a CI engine is a measure of the quantity of oxygen available in the charge-voidage section, it can be deduced that the amount of oxygen at the charge-voidage was either very low or almost insignificant thus causing no or slow diffusion of oxygen. Again, this may also suggest efficient air consumption by the engine at engine loads greater than 31%.

Based on the results in Table 7, the cetane number of the HCNG+10% MB hybrid fuel as determined by ASTM D613, is 50 which falls within the acceptable standard range (48–55) for diesel fuels (Ayoola et al., 2018; Emetere et al., 2020).

4. Conclusion

The combustion, emission and performance characteristics of Moringa diesel admixed Hydrogen-Compressed natural gas (HCNG) in a CI engine have been successfully tested and other significant findings are as follows:

- the engine BTE, HRR and combustion pressure of the Petter PH1 W diesel engine were substantially improved by the fuel blends. Also, the exhaust emissions such as HC, CO, CO_2, O_2 and NOx gases were significantly reduced by the presence of the MB in HCNG.
- the mixed fuels gave higher peak cylinder pressures than the unblended HCNG fuel which confirms the suitability of MB as a very promising additive for CNG since the increment in %MB below the optimum requirement in the fuel mix, does not pose any form of danger to the engine structure.
- the combustion duration for the mixed fuels were longer at low engine loads, but shorter at high engine loads. Consequently, the fuel blends gave higher brake thermal efficiencies when compared to those obtained for the unblended HCNG.
- the optimum MB–HCNG fuel blend for the best engine performance, was found to be the mixture containing 10% MB. Hence, it is advisable to stick to this MB–HCNG blend for engines running on fuel blends of similar compositions. At high engine loads of 58%–100%, higher BTEs ranging from 19–33.9% were obtained for the fuel-blends relative to those of the unblended HCNG fuel whose BTE values were in the range of 15.1%–19%; this justifies the suitability of MB as a viable additive for enhancing the brake thermal efficiency of CI engines.
- the differences in auto ignition temperatures and densities of the hydrogen (858 K and 0.07 g/L) + CNG (813 K with a density 0.7 of g/L) as compared to those of Moringa biodiesel (798 K and 0.882 g/L) were responsible for the rise in the crank angle and pressure which in turn reduced the flash point towards ensuring quick vaporization of the biofuel.
- at maximum (100% engine-load), the 10% MB fuel-blend gave the lowest NOx gas emissions (i.e. 5.01–3.77 gram gas/kg diesel). CO_2 emissions decreased by 11.9% for sample D, 9.5% for sample E, and 8.7% for samples C and B when compared with 'CO_2 emissions of the unblended HCNG sample (sample A). Fuel samples D and E gave close CO_2 emissions (i.e. 2000 g CO_2/kg MB–HCNG, while sample D produced the least CO_2 emissions which range from 1750 g/kg fuel at 20% - 2020 g/kg diesel at 100% engine load; under similar engine load conditions, the unblended HCNG fuel gave 2106 g CO_2/kg fuel at 19% and 2520 g CO_2 /MB–HCNG at 100% engine load which gives a difference of 500 g CO_2/kg MB–HCNG at maximum engine load. The HC emissions, range from 64–46 g/kg fuel for the 10% MB-fuel relative to 85%–65% for the conventional fuel at minimum to full load condition. For fuel blend D, the corresponding NO emissions range from 5.01–3.11%, CO_2 emissions from 1750–2020 g/kg fuel, CO emissions from 64–43 g/kg fuel at minimum (20%) to maximum load conditions (100%); these values are lower compared to the HC emission (85–65 g/kg fuel), NO emission (21–16 g/kg fuel), CO_2 emission (2106–2520) and CO emission (83–56 g/kg fuel) for the conventional fuel, respectively. Furthermore, the oxygen emissions were in the range of 21–11 g/kg fuel for fuel sample D which is also lower relative to that of the conventional fuel (i.e. 34–20 g/kg fuel) for engine load of 20%–31%.

CRediT authorship contribution statement

Babalola Aisosa Oni: Conceived the idea, Carried out the experimentation, Made the first draft copy of the manuscript. **Samuel Eshorame Sanni:** Made useful contributions at different stages of the research, Involved in recomposing key sections of the manuscript, results discussion and general editing of manuscript. **Anayo Jerome Ibegbu:** Made very vital/useful observations at the experimental design and experimentation stages. **Ameloko Anthony Aduojo:** Data curation, Result analyses.

Declaration of competing interest

The authors declare that they have no known competing financial interests or personal relationships that could have appeared to influence the work reported in this paper.

Data availability

All data required for reproducing this research are contained in this manuscript.

Acknowledgements

Authors wish to appreciate Covenant University for supporting this research at the experimental phase and sincerely appreciate OBA1 group auto Services Limited, Benin City, Nigeria for their immense support in the course of carrying out this research.

Funding statement

This research received no funding from any Governmental or non-Governmental organizations as well as not-for-profit organizations

Appendix A. Supplementary data

Supplementary material related to this article can be found online at https://doi.org/10.1016/j.egyr.2021.01.019.

References

Adt, R.R., Swain, M.R., 1974. The hydrogen/methanol–air breathing automobile engine. In: The Hydrogen Economy Miami Energy Conference, 18–20 March, Miami Beach, USA, p. S10-38–48.

Aklouche, F.Z., Loubar, K., Bentebbiche, A., Awad, S., Tazerout, M., 2018. Predictive model of the diesel engine operating in dual-fuel mode fuelled different gaseous fuels. Fuel 220, 599–606. http://dx.doi.org/10.1016/j.fuel.2018.02.053.

Ali, M., Naqvi, B., Watson, I.A., 2018. Possibility of converting indigenous Salvadora Persica L. Seed oil into biodiesel in Pakistan. Int. J. Green Energy 15 (7), 427–435. http://dx.doi.org/10.1080/15435075.2018.1472603.

Alrazen, A.H., Ahmad, K.A., 2018. HCNG Fueled spark ignition (SI) engine with effects on performance and emissions. Renew. Sustain. Energy Rev. 82, 324–342.

Anon, 2014. Report on priority measures to reduce air pollution and protect public health. EPCA Report No. 47, February 2014, Environmental Pollution Prevention Authority, India.

Anon, 2020. Octane and cetane ratings - your guide to diesel fuel and gasoline's specs – auto evolution. https://www.autoevolution.com/news/octane-and-cetane-ratings-ship-launches-boasts-incredible-amenities. (Accessed 23 December 2020).

Arat, H.T., Aydin, K., Baltacioğlu, E., Yaşar, E., Kaan, M.B., Conker, C., Burga, A., 2013. A review of hydrogen-enriched compressed natural gas (HCNG)-fuel in 44 44 diesel engines. J. Macro Trends Energy Sustain. 1 (1), 115–122.

Atabani, A.E., Silitonga, A.S., Ong, H.C., Mahlia, T.M.I., Masjuki, H.H., Badruddin, I.A., et al., 2013. Nonedible vegetable oils: a critical evaluation of oil extraction, fatty acid composition, biodiesel production, characteristics, engine performance and emissions production. Renew. Sustain. Energy Rev. 18, 211–245.

Ağbulut, U., Sarıdemir, S., Albayrak, S., 2019. Experimental investigation of combustion, performance and emission characteristics of a diesel engine fuelled with diesel–biodiesel–alcohol blends. J. Braz. Soc. Mech. Sci. Eng. 41, 389. http://dx.doi.org/10.1007/s40430-019-1891-8.

Ayoola, A.A., Adeniyi, D.O., Sanni, S.E., Osakwe, K.I., Jato, J.D., 2018. Investigating production parameters and impacts of potential emissions from soybean biodiesel stored under different conditions. Environ. Engrg. Res. 23 (1), 54–61. http://dx.doi.org/10.4491/eer.2017.042.

Banapurmath, N.R., Tewari, P.G., 2009. Comparative performance studies of a 4-stroke CI engine operated on dual fuel mode with producer gas and honge oil and its methyl ester (HOME) with and without carburettor. Renew. Energy 34, 1009–1015.

Boretti, A., 2018. Super turbocharging the direct injection diesel engine. Nonlinear Eng. 7, 17–27.

Boretti, A., 2019. Half/full toroidal, single/double roller, CVT based transmission for a super-turbo-charger. Proc. Eng. Technol. Innov. 11, 1–11.

Boretti, A., 2020. Advances in diesel-LNG internal combustion engines. Appl. Sci. 10 (4), 1296. http://dx.doi.org/10.3390/app10041296.

Carlucci, A.P., de Risi, A., Laforgia, D., Naccarato, F., 2008. Experimental investigation and combustion analysis of a direct injection dual-fuel diesel-natural gas engine. Energy 33, 256–263.

Das, L.M., 1996. Utilization of hydrogen e CNG blends in an internal combustion engine. In: 11th World Hydrogen Energy Conference, Stuttgart, Germany, pp. 1513-1535.

Emetere, M.E, Jack-Quincy, S., Aro, S.I., Okonkwo, O.D., Owoeye, F.T., Sanni, S.E., 2020. Validation of biodiesel quality of monodora myristica and moringa oleifera using regression and error analysis of UV absorption results. Biofuels 11 (2), 163–173. http://dx.doi.org/10.1080/17597269.2017.1345362.

Francfort, J., Karner, D., 2006. Hydrogen ICE Vehicle Testing Activities. SAE, 2006-01-0433.

Ghazal, O.H., 2013. Performance and combustion characteristic of CI engine fueled with hydrogen enriched diesel. Int. J. Hydrogen Energy 38, 15469–15476.

Jian, X., Xin, Z., Jianhua, L., Longfei, F., 2010. Experimental study of a single cylinder engine fuelled with natural gas- hydrogen mixtures. Int. J. Hydrogen Energy 35 (2010), 2909–2914.

Kahraman, N., Ceper, B., Akansu, S.O., Aydin, K., 2009. Investigation of combustion characteristics and emissions in a spark-ignited engine fuelled with natural gas and hydrogen blends. Int. J. Hydrogen Energy 34, 1026–1034.

Lather, R.S., Das, L.M., 2019. Performance and emission assessment of a multi-cylinder s.i engine using CNG & HCNG as fuels. Int. J. Hydrogen Energy 44 (38), 21181–21192.

Luo, S., Ma, F., Mehra, R.K., Huang, Z., 2019. Deep insights of HCNG engine research in China. Fuels.

Malogorzata, P., 2014. Mitigation of Landfill Gas Emissions. Taylor and Francis, ISBN: 0415630770.

Mehra, R.K., Duan, H., Juknelevicius, R., Ma, F., Li, J., 2017. Progress in hydrogen enriched compressed natural gas (HCNG) internal combustion engines e a comprehensive review. Renew. Sustain. Energy Rev. 80, 1458–1498.

Montoya, J.P.G., Amell, A.A., Olsen, B.D., 2016. Prediction and measurement of the critical compression ratio of methane number for blends of biogas with methane, propane, and hydrogen. Fuel 186, 168–175.

NGV Global, 2019. Current natural gas vehicle statistics. Available online: www.iangv.org/current-ngvstats. (Accessed on 16 December 2019).

Niju, S., Anushya, C., Balajii, M., 2018. Process optimization for biodiesel production from Moringa Oleifera oil using conch shells as heterogeneous catalyst. Environ. Prog. Sustain. Energy 1–12. http://dx.doi.org/10.1002/ep.13015.

Nwafor, O.M.I., 2003. Combustion characteristics of dual-fuel diesel engine using pilot injection ignition. Inst. Eng. (India) J. 84 (2003), 22–25.

Orhan, A., Zafer, D., Nafiz, K., Veziroglu, T., 2004. Internal combustion engines fueled by natural gas hydrogen mixtures. Int. J. Hydrogen Energy 29 (14), 1527–1539.

Papagiannakis, R.G., Rakopoulos, C.D., Hountalas, D.T., Rakopoulos, D.C., 2010. Emission characteristics of high speed, dual fuel, compression ignition engine operating in a wide range of natural gas/diesel fuel proportions. Fuel 89, 1397–1406.

Park, C., Kim, C., Choi, Y., 2012. Power output characteristics of hydrogen-natural gas blend fuel engine at different compression ratios. Int. J. Hydrogen Energy 37, 8681–8687.

Rashed, M.M., Kalam, M.A., Masjuki, H.H., Mofijur, M., Rasul, M.G., Zulkifli, N.W.M., 2016a. Performance and emission characteristics of a diesel engine fuelled with palm, jatropha, and moringa oil methyl ester. 79, 70–76. http://dx.doi.org/10.1016/j.indcrop.2015.10.046.

Renny, A., Janardan, S., 2008. Hydrogen CNG Blend Performance in a Three-Wheeler. SAE, 28-0119.

Shrestha, S., Karim, G., 1999. Hydrogen as an additive to methane for spark ignition engine applications. Int. J. Hydrogen Energy 24, 577–586.

Sierens, R., Verhelst, S., 2001. Hydrogen fuelled V-8 engine for city bus application. Int. J. Hydrogen Energy 2, 39–45.

Sirens, R., Rosseel, E., 2000. Variable composition hydrogen/ natural gas mixtures for increased engine efficiency and decreased emissions. J. Eng. Gas Turbines Power 122, 135–140.
Srinivasan, K.K., Krishnan, S.R., Qi, Y., Midkiff, K.C., Yang, H., 2007. Analysis of diesel pilot ignited natural gas low-temperature combustion with hot exhaust gas recirculation. Combust. Sci. Technol. 179 (9), 1737–1776.
Swain, M.R., Yusuf, M.J., Dulger, Z., Swain, M.N., 1993. The Effects of Hydrogen Addition on Natural Gas Engine Operation. SAE, 932775.
Wang, Z., Du, G., Wang, D., Xu, Y., Shao, M., 2018. Combustion process decoupling of a diesel/natural gas dual-fuel engine at low loads. Fuel 232, 550–561.
Yousefi, A., Guo, H., Birouk, M., 2019. E_ect of diesel injection timing on the combustion of natural gas/diesel dual-fuel engine at low-high load and low-high speed conditions. Fuel 235, 838–846.
Zhang, Q., Xu, Z., Li, M., Shao, S., 2016. Combustion and emissions of a Euro VI heavy-duty natural gas engine using EGR and TWC. J. Nat. Gas Sci. Eng. 28, 660–671.
Zheng, J., Wang, J., Zhao, Z., Wang, D., Huang, Z., 2019. Effect of equivalence ratio on combustion and emissions of a dual-fuel natural gas engine ignited with diesel. Appl. Therm. Eng. 14, 738–751.